CrystEngComm

Cite this: *CrystEngComm*, 2011, **13**, 4861

www.rsc.org/crystengcomm

PAPER

Help nanorods "stand" on microsubstrate to form hierarchical ZnO nanorod-nanosheet architectures

Jun Jiang,[a] Feng Gu,*[a] Wei Shao,[a] Lili Gai,[a] Chunzhong Li*[a] and Guangjian Huang[b]

Received 8th February 2011, Accepted 20th April 2011
DOI: 10.1039/c1ce05180f

ZnO nanorods were helped to "stand" vertically on microsubstrates by an interesting seed-mediated approach. Taking ZnO nanosheets as the microsubstrates, ZnO nanorods can grow vertically, not lying horizontally, on the facets with the aid of a seed layer precoating to form hierarchical ZnO nanorod-nanosheet architectures. The diameter as well as the length of the standing nanorods can be controlled effectively by adjusting the growth time and ammonia amount in the growth solution. The precoated seed layer has been found to be the key factor in determining the resultant morphology. Room-temperature photoluminescence studies revealed that the near band-edge (NBE) emission intensity of the hierarchical architectures was increased greatly compared with that of bare ZnO nanosheets. These special hierarchical architectures make them appealing for future microdevice applications.

1. Introduction

Zinc oxide (ZnO) has been extensively studied due to its good optical, electrical, and piezoelectric properties.[1–4] A large number of ZnO nanostructures, such as nanobelts,[5] nanotubes,[6] nanorings,[7] and nanosheets,[8] *etc.*, have been successfully synthesized mainly by gas-phase and solution-phase deposition methods.[9–14] While the gas-phase deposition requires high temperature and specially designed reactors,[15,16] the solution-phase approaches can be carried out facilely and mildly, which recently become the priority that one has frequently taken to fabricate large-scale ZnO nanostructures.[17,18] Among various ZnO nanostructures, hierarchical structures composed of one-dimensional nanostructures can serve as functional building blocks for various nano-device applications, including chemical sensors, light emitting diodes, and solar energy conversion.[19,20] Thus, various hierarchical ZnO structures, such as branched crystallites[2] and nanowires,[21] nanoflowers[22] and so on,[23,24] have been prepared successfully. However, most of them were synthesized mainly depending on gas-phase solution. Since Yang *et al.* reported the synthesis of ZnO nanowire arrays on a sapphire substrate,[25] much effort has been devoted to synthesizing ZnO with oriented nanostructures, because this well aligned structure is a good candidate for photo-electric device applications such as field effect transistor and nanogenerator.[26–29] For example, Cheng *et al.*[30] have synthesized branched ZnO nanowires arrays on an FTO substrate for dye sensitized solar cells, which had a light-to-electricity conversion efficiency that was twice as high as the bare ZnO nanowires array. It should be noted that these structures totally grew on macrosubstrates, *e.g.*, FTO or ITO. However, in order to explore the optoelectric properties of promising microdevices constructed from ZnO nanostructures, it is necessary to assemble those hierarchical ZnO nanostructures into arrays or networks on microsubstrates.[31] Very recently, Xu *et al.*[32] reported the synthesis of hierarchical ZnO nanowire-nanosheet structure by combination of both electro-deposition and chemical bath deposition methods. But the ZnO nanowires were disorderly as grown on the ZnO nanosheets, which was not the ideal structure for future microdevices and may degrade the device performance. A power conversion efficiency of 4.8% was obtained. Therefore, from these progresses, we can find it is necessary to study the related fundamental issues on how to control morphology, orientation and surface architectures of ZnO nanostructures on microsubstrates to form hierarchical ZnO nanostructures for future microdevice applications.

In this work, we developed a facile method to "help" ZnO nanorods stand on the nanosheets to form well-structured hierarchical ZnO nanorod-nanosheet architectures. By introducing a seed layer on the primary nanosheets, the ZnO nanorods can grow on the facets of ZnO nanosheets perpendicularly with good alignment. The orientation, diameter as well as length of the nanorods can be controlled effectively.

2. Experimental

2.1 Sample preparation

The formation of ZnO nanosheets on FTO was followed as the literature described.[33] In a typical procedure, an aqueous solution of 0.05 M zinc nitrate hexahydrate (china-reagent) and

[a]*Key Laboratory for Ultrafine Materials of Ministry of Education, School of Materials Science and Engineering, East China University of Science and Technology, Shanghai 200237, China. E-mail: czli@ecust.edu.cn; gufeng@ecust.edu.cn; Fax: +86-21-64250624*
[b]*Department of Surgery, Huashan Hospital, Fudan University, Shanghai 200040, China*

1.0 M urea (Shanghai Ling-Feng Ltd.) were used. Nitric acid was added to the solution to adjust the initial pH value to 4. Then cleaned FTO (Nippon Sheet Glass, SnO_2: F, 15 ohm sq^{-1}) substrate was put into the bottles filled with solution and sealed up, and was kept still at 80 °C for 24h in an oven. After deposition, the obtained films were rinsed with water and dried at 80 °C overnight. For preparation of primary ZnO nanosheets, the above films were annealed at 350 °C for 20 min. For the preparation of seeded ZnO nanosheets, the above films were wet with a droplet of 0.005 M acetate dihydrate in ethanol, rinsed with clean ethanol after 10 s, then blown dry with a stream of air. This coating step is repeated three times, and annealed at 350 °C for 20 min. Then, the hierarchical ZnO nanowire-nanosheet architectures were formed by immersing the primary nanosheets or seeded nanosheets in 50 ml of aqueous solution containing 0.05 M zinc nitrate (china-reagent), 0.05 M hexamethylenetetramine (Shanghai Ling-Feng Ltd.), 0.005 M polyethyleneimine (Mn ~ 1200, Sigma) and 0–2.5 ml ammonia water (25–28 wt%, Shanghai Ling-Feng Ltd.) at 90 °C for 10 min–24 h. The obtained hierarchical nanorod-nansheet architectures were finally rinsed with water and ethanol, and then annealed at 450 °C for 30 min.

2.2 Characterization

The general morphology and crystallinity of the samples were examined by scanning electron microscopy (SEM; Hitachi S-4800), high-resolution transmission electron microscopy (HRTEM, JEM-2010) and X-ray diffraction (XRD; Rigaku D/max 2550). The absorptions of the samples were measured with a spectrophotometer (UV-vis; Varian ltd. Cary-500 spectrometer). The PL measurements were performed on the luminescence spectrophotometer (Fluorolog-3-p) with Xe lamp emitting at 325 nm as excitation source at room temperature.

3. Results and discussion

ZnO nanosheets were taken as the microsubstrates in this work. By pre-coating a seed layer, the ZnO nanorod arrays stood vertically and symmetrically on both facets of the nanosheets with a diameter of ~60 nm and length of 540 nm, respectively (Fig. 1a). However, without pre-coating a seed layer, a disordered nanorod-nanosheet structure was obtained (Fig. 1b). ZnO nanorods with diverse diameters ranging from 20–80 nm were randomly and disorderly grown on the surfaces of unseeded nanosheets (the inset of Fig. 1b). The crystallinity of the samples was studied by XRD (Fig. 1c). Several peaks were distinctly recorded to be centered at 31.9, 34.5, 36.3, 47.6, 56.7°, respectively. All these diffraction peaks are in good agreement with wurtzite type ZnO with cell parameters $a = 3.249$ Å and $c = 5.206$ Å (JCPDF no. 36-1451). In addition, the intensity of the diffraction peaks of the hierarchical ZnO nanorod-nanosheet architectures are much stronger than those of bare ZnO nanosheets, which can be ascribed to the good crystallinity of the large quantity of ZnO nanorods formed on the nanosheets.

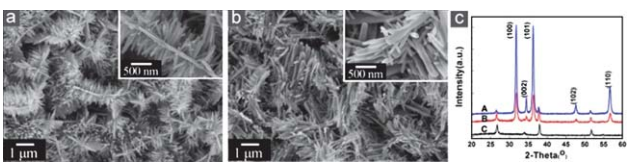

Fig. 1 SEM images of hierarchical ZnO nanorod-nanosheet architectures derived from (a) seeded ZnO nanosheets (Sample C) and (b) unseeded nanosheets. (c) XRD patterns of the samples: (A) ZnO nanorod-nanosheet architectures, (B) seeded ZnO nanosheets, (C) FTO substrates.

The structure and morphology of the hierarchical ZnO nanorod-nanosheet architectures can be readily controlled by tuning the size of the ZnO nanorods. As is well known, the growth feature of ZnO nanorods are affected by several parameters, such as precursor concentration, pH, growth temperature, growth time, kinds of additives, *etc.*[34] In the present study, the size of the ZnO nanorods can be controlled simply by adjusting the growth time and ammonia amount. These parameters and their influence on the diameter and length of the ZnO shell are listed in Table 1. In the absence of ammonia, only a small number of tiny ZnO crystallites attached to the surface of the nanosheets (Fig. 2a), which can be ascribed to slow heterogeneous nucleation rate during the high supersaturation degree in the growth solution.[35] Once ammonia was added, the supersaturation degree decreased effectively. As a result, the growth rate of the ZnO nanorods was increased greatly. For example, when the amount of ammonia was increased from 1.5 ml to 2.5 ml, the size of the ZnO nanorods would change from 40 nm × 230 nm to 180 nm × 1180 nm (Table 1 and Fig. 2b,c). In this case, the big size and high density of the ZnO nanorods buried the nanosheet totally and we can't find the nanosheets beneath (Fig. 2c). When the reaction time was 10 min, tiny ZnO nanorods/nanoparticles began to germinate on the surfaces of the primary ZnO nanosheets (Fig. 2d). When we increased the reaction time from 1 h to 24 h, a large quantity of ZnO nanorods uniformly and vertically rooted in ZnO nanosheets outstretched to fill the intervals between the nanosheets and the size of the ZnO nanorods increased from 70 nm × 460 nm to 80 nm × 860 nm (Table 1 and Fig. 2e,f).

To investigate why the nanorods stand on the nanosheets to form this kind of hierarchical ZnO architecture, a detailed structural characterization is desired. During the synthetic process, the key factor determining the resultant morphology, lying or standing, is the seeds pre-coated on the nanosheets. It is known that the orientation of ZnO nanorods is primary determined by the nucleation and growth of the first few layers of zinc and oxygen atoms. Yang *et al.*[36] have demonstrated that the acetate-derived seeds are flat platelets, 25–40 atomic thick in the {001} orientation and *c*-axis alignment, leading to vertical oriented growth of ZnO nanorods on sapphire substrates. In our work, HRTEM images were taken to investigate the

Table 1 Summary of the experimental conditions and results of the obtained samples

Sample	A	B	C	D	E	F	G
Ammonia (ml)	0	1.5	2	2.5	2	2	2
Time (h)	3	3	3	3	1/6	1	24
Diameter (nm)	40	40	60	180	40	70	80
Length (nm)	60	230	540	1180	70	460	860

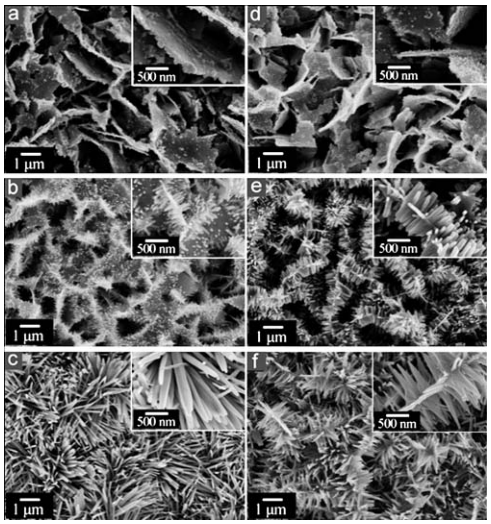

Fig. 2 SEM images of the hierarchical ZnO nanorod-nanosheet architectures: (a) Sample A, (b) Sample B, (c) Sample D, (d) Sample E, (e) Sample F, (f) Sample G.

microstructure of the interfacial region of the ZnO nanorod and nanosheet for better understanding the crystal growth behavior. After 10 min growth, tiny ZnO rod arrayed on the sheet (Fig. 3a), implying that ZnO nanorods were anchored to the sheet perpendicularly since the initial stage based on the preferential growth along the [001] direction was induced by the seeds with {001} facets normal to the sheet. From HRTEM images, the lattice spacing of ~0.52 nm can be ascribed to the ZnO (001) crystal planes, confirming its preferential growth direction is [001]. The ED pattern also confirmed a single crystalline nature of the nanorod (Fig. 3c). It should be noted that the lattice continuity at the interfacial region of the nanorod and nanosheet is clearly observed, showing perfect structural accord, which will facilitate electron transfer and better electron collection efficiency can be expected. In our case, $Zn_4CO_3(OH)_6 \cdot H_2O$ nanosheets were first prepared in a large scale by a simple chemical deposition reaction (Fig. 4a). After the $Zn_4CO_3(OH)_6 \cdot H_2O$ nanosheets were wetted with acetate dehydrate ethanol solution and followed with thermal decomposition at 350 °C, aligned acetate-derived seeds were formed (Fig. 4b). As a result, the ZnO nanorods derived from those aligned seeds on the seeded nanosheets are vertical in orientation and uniform in size. For the primary ZnO nanosheets, though no seeds were coated, the ZnO nanoparticles that existed on the sheets' surface can still act as seeds for the following nanorod growth. However, it should be

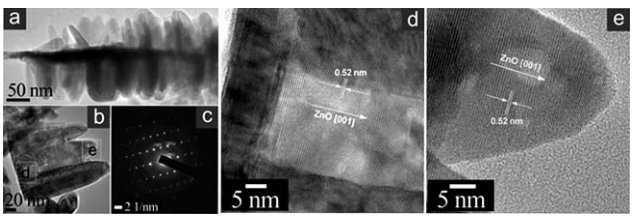

Fig. 3 TEM image of the hierarchical ZnO architecture after 10 min growth (a, b). SAED pattern of the tip of one rod shown in (b). (d, e) HRTEM images corresponding to squares d, e in (b).

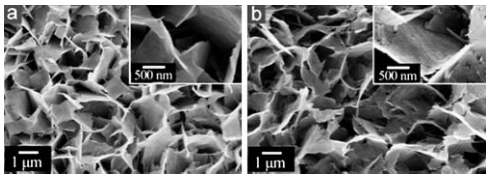

Fig. 4 SEM images of (a) $Zn4CO_3(OH)_6 \cdot H_2O$ nanosheets and (b) seeded ZnO nanosheets.

noted that the ZnO nanoparticles rest at random angles with the *c*-axis, resulting in disordered growth, not vertical growth, of ZnO nanorods. Moreover, as the size of the ZnO nanoparticle is not uniform, the ZnO nanorods with different sizes are randomly rooted on the surfaces of the nanosheets.

In this work, the size of the ZnO nanorods was found to be dependent on the ammonia amount used. As is well known, in chemical bath deposition, ZnO nanorods are synthesized based on following reaction:[35]

$$Zn^{2+} + 2OH^- \rightarrow Zn(OH)_2 \rightarrow ZnO + H_2O \quad (1)$$

or

$$Zn^{2+} + 2OH^- \rightarrow ZnO + H_2O \quad (2)$$

where HMTA or NaOH was used as the hydroxide source. When no ammonia was added, the supersaturation degree was very high, leading to a fast homogeneous nucleation rate. Only a small quantity of ZnO crystallites grew on the nanosheets with slow heterogeneous nucleation rate. When a small amount of ammonia was added, the solution became turbid due to the formation of $Zn(OH)_2$ precipitates. The turbid solution became clear again by increasing the ammonia amount. It is known that ammonia forms complexes with zinc ions as the following reaction[37]:

$$Zn^{2+} + 4NH_3 \rightarrow Zn(NH_3)_4{}^{2+} \quad (3)$$

$$Zn(NH_3)_4{}^{2+} + 2OH^- \rightarrow ZnO + 4NH_3 + H_2O \quad (4)$$

These complexes can serve as a buffer for Zn^{2+}, and it continuously supplies Zn^{2+} while lowering the degree of supersaturation of the growth solution. The $Zn(NH_3)_4{}^{2+}$ complex reacts with hydroxide and produces ZnO at a suitable reaction temperature. In this case, heterogeneous nucleation will take place preferentially on the ZnO seeds present on the nanosheets, and well-aligned ZnO nanorods will be formed. Increasing the amount of ammonia would lead to the formation of more $Zn(NH_3)_4{}^{2+}$ complexes. Therefore, the homogeneous nucleation rate is retarded effectively, resulting in a faster growth rate of ZnO nanorods. As a result, the size of the ZnO nanorods, diameter and length, was obviously increased by increasing ammonia amount. However, if excess ammonia was added, the heterogeneous nucleation would be hindered due to high pH degree.

UV-vis absorption spectra of the hierarchical ZnO nanorod-nanosheet architectures and the seeded ZnO nanosheets are shown in Fig. 5. The absorption onset appears blue-shifted upon the formation of hierarchical ZnO nanorod-nanosheet

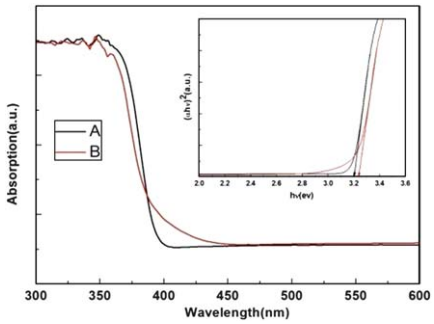

Fig. 5 Absorption spectra of (a) the seeded ZnO nanosheets and (b) the hierarchical ZnO nanorod-nanosheet architectures (Sample G).

architectures. The blue shift of absorption onset can be ascribed to the enhanced surface effect due to a large surface-to-volume ratio of the hierarchical ZnO architectures, even though the size of ZnO nanorod is larger than that of exciton Bohr radius.[38] Previous work also reported a similar blue shift of hierarchical structured ZnO samples with secondary ZnO structures grown on the surfaces of ZnO nanorods.[23] The band gap energy for the ZnO can be determined by the following formula:[14,39]

$$\alpha = \frac{K(h\nu - E_g)^{n/2}}{h\nu},$$

where α is the absorption coefficient, K is a constant, E_g is the band gap, and n is equal to 1 for a direct transition. The band gap can be estimated from a plot of $(\alpha h\nu)^2$ *vs.* photon energy. The intercept of the tangent to the plot will give a good approximation of the band gap energy for this direct band gap material. From the inset of Fig. 5, the band gaps for the seeded ZnO nanosheet and hierarchical ZnO nanorod-nanosheet architectures are 3.21 eV and 3.24 eV, respectively, close to the band gap for bulk ZnO. This can be ascribed to the big size of the architecture and the nanosheets. In addition, compared with the nanosheets, the ZnO nanorod-nanosheet architectures exhibit better absorption in the range of 400–450 nm, which ascribed to the enhanced light scattering effect.

Fig. 6 shows the room temperature PL spectra of the ZnO nanosheets and the hierarchical ZnO nanorod-nanaosheet architectures with nanorods with size of 40 × 70 nm, 60 × 540 nm and 80 × 860 nm (Table 1). Strong emission peaks

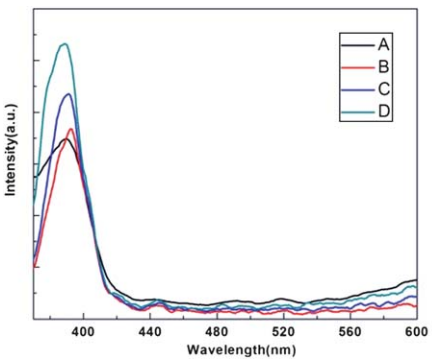

Fig. 6 PL spectra of (a) seeded ZnO nanosheets and ZnO nanorod-nanosheet architectures, b) Sample E, c) Sample C, d) Sample G.

at ~390 nm were observed for all samples, which generally correspond to the near band-edge (NBE) emission resulting from the recombination of free excitons.[40–42] In addition, a weak green emission peak at ~520 nm was observed for the seeded ZnO nanosheets, which can be generally attributed to the deep-level defect recombination.[43] Once the hierarchical ZnO nanorod-nanosheet architectures were formed, the NBE emission intensity was increased greatly, whereas the green emission intensity was decreased compared with that of the ZnO nanosheets (Fig. 6a). The sharp NBE emission and weak deep-level emission peaks indicate that the hierarchical ZnO nanorod-nanosheet architectures have a low defect concentration and better optical properties with potential applications in optoelectronic devices. The blue shift of the NBE emission peak of the hierarchical ZnO nanorod-nanaosheet architectures can be ascribed to the better crystallinity of the structures with increased nanorod size. In addition, the NBE emission intensity of the hierarchical ZnO nanorod-nanosheet architectures was increased gradually with the size of the nanorods, which is consistent with the XRD results.

4. Conclusions

In summary, interesting hierarchical ZnO nanorod-nanosheet architectures have been demonstrated with ZnO nanorods standing vertically on nanosheets using a facile chemical bath deposition method. By taking advantage of pre-coating a seed layer on the primary nanosheets, the orientation, diameter as well as length of the nanorods can be controlled effectively. The pre-coated seeds are in {0001} orientation and c-axis alignment, which can determine the crystal growth direction and help the nanorods stand on the nanosheets' facets. Without the precoating of the seed layer, the nanorods can be formed as before, but not standing, instead they are lying on the facets. Stronger NBE emission from the hierarchical ZnO architectures was exhibited, with the size of nanorods, due to better crystallinity. These hierarchical ZnO nanorod-nanosheet architectures may find potential for microdevice applications with novel optoelectric properties.

Acknowledgements

This work was supported by the National Natural Science Foundation of China (20925621, 81071994), Shanghai Rising-Star Program (09QH1400700, 09QA1401500), Special Projects for Key Laboratories in Shanghai (09DZ2202000, 10DZ2211100), Special Projects for Nanotechnology of Shanghai (0952nm02100), Program of Shanghai Subject Chief Scientist (09XD1400800), and Basic Research Program of Shanghai (10JC1403300).

Notes and references

1 U. Ozgur, Y. I. Alivov, C. Liu, A. Teke, M. A. Reshchikov, S. Dogan, V. Avrutin, S. J. Cho and H. Morkoc, *J. Appl. Phys.*, 2005, **98**.
2 T. Zhang, W. Dong, M. Keeter-Brewer, S. Konar, Roland N. Njabon and Z. Ryan Tian, *J. Am. Chem. Soc.*, 2006, **128**, 10960–10968.
3 J. P. Liu, X. T. Huang, K. M. Sulieman, F. L. Sun and X. He, *J. Phys. Chem. B*, 2006, **110**, 10612–10618.
4 J. H. He, C. L. Hsin, J. Liu, L. J. Chen and Z. L. Wang, *Adv. Mater.*, 2007, **19**, 781–784.

5 X. D. Wang, Y. Ding, C. J. Summers and Z. L. Wang, *J. Phys. Chem. B*, 2004, **108**, 8773–8777.
6 J. J. Qiu, W. D. Yu, X. D. Gao and X. M. Li, *Nanotechnology*, 2006, **17**, 4695–4698.
7 W. L. Hughes and Z. L. Wang, *Appl. Phys. Lett.*, 2005, **86**, 043106.
8 M. Mo, J. C. Yu, L. Z. Zhang and S. K. A. Li, *Adv. Mater.*, 2005, **17**, 756–760.
9 Z. W. Pan, Z. R. Dai and Z. L. Wang, *Science*, 2001, **291**, 1947–1949.
10 S. Jebril, H. Kuhlmann, S. Muller, C. Ronning, L. Kienle, V. Duppel, Y. K. Mishra and R. Adelung, *Cryst. Growth Des.*, 2010, **10**, 2842–2846.
11 H. Yan, R. He, J. Johnson, M. Law, Richard J. Saykally and P. D. Yang, *J. Am. Chem. Soc.*, 2003, **125**, 4728–4729.
12 B. Liu and H. C. Zeng, *J. Am. Chem. Soc.*, 2004, **126**, 16744–16746.
13 H. Jiang, J. Q. Hu, F. Gu and C. Z. Li, *J. Alloys Compd.*, 2009, **478**, 550–553.
14 F. Gu, S. F. Wang, M. K. Lu, G. J. Zhou, D. Xu and D. R. Yuan, *Langmuir*, 2004, **20**, 3528–3531.
15 C. Cheng, M. Lei, L. Feng, T. L. Wong, K. M. Ho, K. K. Fung, Michael M. T. Loy, D. Yu and N. Wang, *ACS Nano*, 2009, **3**, 53–58.
16 A. Cao, G. Meng and P. Ajayan, *Adv. Mater.*, 2004, **16**, 40–44.
17 J. Zhang, L. D. Sun, J. L. Yin, H. L. Su, C. S. Liao and C. H. Yan, *Chem. Mater.*, 2002, **14**, 4172–4177.
18 L. E. Greene, B. D. Yuhas, M. Law, D. Zitoun and P. Yang, *Inorg. Chem.*, 2006, **45**, 7535–7543.
19 C.-H. Chen, S.-J. Chang, S.-P. Chang, M.-J. Li, I. C. Chen, T.-J. Hsueh, A.-D. Hsu and C.-L. Hsu, *J. Phys. Chem. C*, 2010, **114**, 12422–12426.
20 M. Krunks, A. Katerski, T. Dedova, I. O. Acik and A. Mere, *Sol. Energy Mater. Sol. Cells*, 2008, **92**, 1016–1019.
21 J. Y. Lao, J. G. Wen and Z. F. Ren, *Nano Lett.*, 2002, **2**, 1287–1291.
22 D. F. Zhang, L. D. Sun, J. Zhang, Z. G. Yan and C. H. Yan, *Cryst. Growth Des.*, 2008, **8**, 3609–3615.
23 J. Liu, Z. Guo, F. Meng, Y. Jia, T. Luo, M. Li and J. Liu, *Cryst. Growth Des.*, 2009, **9**, 1716–1722.
24 F. Lu, W. Cai and Y. Zhang, *Adv. Funct. Mater.*, 2008, **18**, 1047–1056.
25 M. H. Huang, S. Mao, H. Feick, H. Yan, Y. Wu, H. Kind, E. Weber, R. Russo and P. Yang, *Science*, 2001, **292**, 1897–1899.
26 Q. Y. Zhang, C. S. Xie, S. P. Zhang, A. H. Wang, B. L. Zhu, L. Wang and Z. B. Yang, *Sens. Actuators, B*, 2005, **110**, 370–376.
27 H. Jiang, J. Q. Hu, F. Gu and C. Z. Li, *Nanotechnology*, 2009, **20**, 5.
28 Y. Qin, R. Yang and Z. L. Wang, *J. Phys. Chem. C*, 2008, **112**, 18734–18736.
29 M. P. Lu, J. Song, M. Y. Lu, M. T. Chen, Y. Gao, L. J. Chen and Z. L. Wang, *Nano Lett.*, 2009, **9**, 1223–1227.
30 H. M. Cheng, W. H. Chiu, C. H. Lee, S. Y. Tsai and W. F. Hsieh, *J. Phys. Chem. C*, 2008, **112**, 16359–16364.
31 T. L. Sounart, J. Liu, J. A. Voigt, M. Huo, E. D. Spoerke and B. McKenzie, *J. Am. Chem. Soc.*, 2007, **129**, 15786–15793.
32 F. Xu, M. Dai, Y. Lu and L. Sun, *J. Phys. Chem. C*, 2010, **114**, 2776–2782.
33 K. Kakiuchi, M. Saito and S. Fujihara, *Thin Solid Films*, 2008, **516**, 2026–2030.
34 K. Yu, Z. Jin, X. Liu, J. Zhao and J. Feng, *Appl. Surf. Sci.*, 2007, **253**, 4072–4078.
35 C. Xu, P. Shin, L. Cao and D. Gao, *J. Phys. Chem. C*, 2010, **114**, 125–129.
36 L. E. Greene, M. Law, D. H. Tan, M. Montano, J. Goldberger, G. Somorjai and P. Yang, *Nano Lett.*, 2005, **5**, 1231–1236.
37 L. L. Yang, Q. X. Zhao, M. Willander, X. J. Liu, M. Fahlman and J. H. Yang, *Cryst. Growth Des.*, 2010, **10**, 1904–1910.
38 M. Yin and S. Brien, *J. Am. Chem. Soc.*, 2003, **125**, 10180.
39 F. Gu, S. F. Wang, M. K. Lu, G. J. Zhou, D. Xu and D. R. Yuan, *J. Phys. Chem. B*, 2004, **108**, 8119–8123.
40 H. Jiang, J. Hu, F. Gu and C. Li, *J. Phys. Chem. C*, 2008, **112**, 12138–12141.
41 X. Wang, Q. Ding, H. Huang and S. Yang, *Phys. Lett. A*, 2007, **365**, 175–179.
42 X. Zhang, D. Liu, L. Zhang, W. Li, M. Gao, W. Ma, Y. Ren, Q. Zeng, Z. Niu, W. Zhou and S. Xie, *J. Mater. Chem.*, 2009, **19**, 962–969.
43 Q. Cheng and K. Ostrikov, *CrystEngComm*, 2011, **xx**, xxx–xxx.